nary artery stenosis. And plaque composition could be clearly differentiated and classified by MSCT, which holds promise for noninvasive risk assessment in patients with known or suspected coronary artery disease.

2:45 p.m.

845-4 Noninvasive Assessment of In-Stent Restenosis by 16-Slice Multislice Computed Tomography

Osamu Kuboyama, Tsunekazu Kakuta, Shigeki Kimura, Taishi Yonetsu, Kenji Suzuki, Yoshitoshi Nagata, Masahiko Goya, Yoshito Iesaka, Hideomi Fujiwara, Mitsuaki Isobe, Tsuchiura Kyodo Hospital, Tsuchiura, Japan, Tokyo Medical and Dental University, Tokyo, Japan

Background: Multislice computed tomography (MSCT) is a promising technique for noninvasive coronary artery assessment. We investigated the potential value of MSCT angiography to noninvasively identify in-stent restenosis and patency.
Methods: We studied 32 stent patients (26 male, 6 female; mean age 64 years), by both MSCT (16x0.75mm detector collimation, 0.42-s rotation time, retrospectively ECG-gated, with additional beta-blockade in 26 patients) and conventional coronary angiography. A total number of 62 stents (39xMultilink, 7xNIR, 6xVelocity, 1xWiktor, 4xGRII, 3xS6, 2xPS) were evaluated at a mean interval of 23 months after implantation. MSCT images of in-stent lumen and adjacent coronary arteries were analyzed by two investigators, unaware of the results of conventional angiography, for in-stent restenosis and patency. The results were compared with conventional angiography. Axial slices, maximum intensity projections, multiplanar, and 3-dimensional volume rendering reconstructions were assessed for image analysis.
Results: All stents were correctly located and 50 stents (80.6%) were evaluable for in-stent lumen and adjacent coronary arteries. Twelve stents were unevaluable (8xMultilink, 1xWiktor, 2xGRII, and 1xNIR) due to stent design, small stent size, severe calcification, and motion artifacts. Using conventional angiography as the gold standard in 50 evaluable stents, MSCT permitted the detection of 11 of 12 significant (>50%) stenoses (sensitivity, 91.7%) and correctly depicted the absence of restenosis in 27 of 38 stents (specificity, 71.1%). These values correspond to positive predictive value of 50% (11 of 22), and negative predictive value of 96.4% (27 of 28). In 11 of 12 angiographically restenotic stents, MSCT correctly identified the type of stenosis (focal in-stent, diffuse in-stent, and edge stenosis).
Conclusion: The latest generation of MSCT is useful in localizing intracoronary stents and may be helpful to noninvasively identify the patients without in-stent restenosis. MSCT may identify the type of in-stent restenosis if image quality is sufficient.

3:00 p.m.

845-5 Assessment of Microvascular Function After Acute Myocardial Infarction by 16-Slice Computed Tomography

Jonathan Lessick, Robert Dragu, Shmuel Rispler, Rafael Beyar, Haim Hammerman, Michael Kopilevitz, Yoram Agmon, Shimon Reisner, Diab Mutlak, Ahuva Engel, Rambam Medical Center, Haifa, Israel

Multislice CT is capable of simultaneously assessing the coronary arteries, myocardial function and myocardial perfusion in a single scan. An additional scan, 5 minutes post-contrast can be added to assess late enhancement (LE), giving additional information concerning microvascular function.
Methods: We scanned 17 patients from day 3 to 7 following an acute myocardial infarction (MI) using a Philips IDT scanner, during injection of 120cc contrast. Of these, 13 underwent a late 5 minute post-contrast scan as well. All patients underwent catheterization with proven patent coronary arteries (Most underwent angioplasty). An echocardiogram was also performed in the 1st week post-MI. Using the 16-segment approach, segments were scored as normal, hypokinetic (hy) or akinetic (ak). Three short axis slices (apex, mid, base) were reformatted for each CT scan after being reconstructed in phases 0%, 40-50% and 70-80%, and were assessed for the presence and degree of early perfusion defects (ED) and LE.
Results: All patients with abnormal contraction on echocardiography demonstrated ED, however notall abnormal segments had ED. Nine of 13 patients had LE. Of 272 segments analysed, 12/35 hy and 28/46 ak segments demonstrated ED, while 7/24 hy and 19/33 ak segments showed LE. Ak segments had a larger area of LE, compared to hypokinetic segments (p=0.04), however ED size and transmurality and LE transmurality were not significantly different. The size of the ED correlated reasonably well with the number of abnormal segments on echocardiogram (r=0.55).
In summary, microvascular function commonly follows acute MI and correlates with the size of the dysfunctional zone and the severity of the dysfunction.

3:15 p.m.

845-6 Anatomical Observations of the Left Atrium and Pulmonary Veins by Multislice Computed Tomography in Patients With Atrial Fibrillation

Monique R.m Jongbloed, Jeroen J. Bax, Martijn S. Dirksen, Ernst E. van der Wall, Albert de Roos, Martin J. Schalij, Leiden University Medical Center, Leiden, The Netherlands

Background: Electrical isolation of pulmonary veins (PV) by radiofrequency catheter ablation (RFCA) at PV ostia may cure atrial fibrillation (AF). Information on ostial shape and insertion is mandatory to determine ablation strategy. No proper definition of the pulmonary venous junction is present at this time.
Methods: MSCT was performed in 33 patients (pts) referred for RFCA at PV ostia. The insertion of PV in the left atrium (LA) was evaluated in 3 orthogonal planes and 3-D reconstructions. The border of the LA was extrapolated on coronal or transversal sections and a virtual line was drawn. If the ostium of the PV was 0.5 cm outside this line, the insertion was defined as "common ostium" (Figure). The sagital plane was used to confirm a common truncal part of superior and inferior PV. PV ostial diameters were measured in 2 directions.
Results: Common ostia of left PV were observed in 26 (79%) pts and of right PV in 11 (33%) pts. Additional left and right PV were observed in 1 and 10 pts respectively. An early branching pattern of PV was observed frequently (67% for left and 85% for right PV). Indices of measurements in 2 directions were 1.39±0.29 vs 1.21±0.17 mm for left and right PV respectively, suggesting an oval shape of especially left PV ostia.
Conclusion: Variation in anatomy occurs in a large number of pts. Common ostia are observed more often in left PV. Additional veins and early branching were seen more often in right PV. Recognition of variations in PV anatomy using a standardized method may facilitate RFCA of PV ostia.

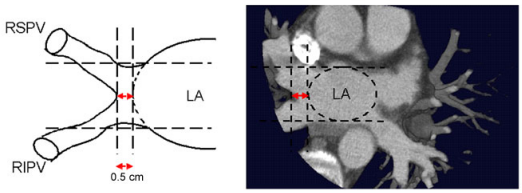

POSTER SESSION

1168 Ultrasound at the Bench

Tuesday, March 09, 2004, 3:00 p.m.-5:00 p.m.
Morial Convention Center, Hall G
Presentation Hour: 4:00 p.m.-5:00 p.m.

1168-161 Effect of High Intensity Focused Ultrasound on Cardiac Valves

Ryo Otsuka, Kumiko Hirata, Kana Fujikura, Yuki Oe, David Engel, Charles Marboe, Marco Di Tullio R. Di Tullio, Robert Muratore, Fred Lizzi, Shunichi Homma, Columbia University, New York, NY, River Side Institute, New York, NY

Backgrounds: High intensity focused ultrasound (HIFU) produces immediate focal lesions with intense focused exposures within short periods. HIFU beams can be noninvasively focused within small volumes. Exposures at high intensity levels in a few seconds produced superficial thermal lesions and creating valvular lesions may prove to be useful for such procedures as valvuloplasty or valvuloplasty. The purpose of this study was to evaluate the possibility to create lesions in valve tissues in-vitro.
Methods: We studied 10 calf mitral valves. Each specimen was mounted on rubber sheet and immersed in a water bath at 37 C. The focal point was set at 2.5 cm from the transducer. The operating frequency of the transducer was 4.67 MHz, and the focal zone was10mm depth × 1.1 mm wide. Ultrasound energy was applied with an acoustic intensity of 26.9kW/cm^2 for 10 seconds, 20 sec, 30 sec, 40 sec, 50 sec and 60 sec on each valve.
Results: Visible changes of the valves required more than 20 second exposure at this intensity. The surfaces of lesion on mitral valve were slightly discolored, and pathologically coaglation of tissue in the affected areas were observed. HIFU exposure for more than 40 sec resulted in perforation on all leaflets with mean diameter of 1.0±0.2 mm.
Conclusion: We concluded that HIFU could create superficial thermal lesions and perforation in mitral valve tissues. With further refinement, HIFU may prove useful for valvulotomy or valvuloplasty.

1168-162 Targeted Ablation of Myocardium Using High Intensity Focused Ultrasound in Beating Dog Hearts

Ryo Otsuka, Kana Fujikura, Todd Pulerwitz, Kumiko Hirata, Jie Wang, Daniel Burkhoff, Robert Muratore, Fred Lizzi, Shunichi Homma, Columbia University, New York, NY, River Side Institute, New York, NY

Backgrounds: High intensity focused ultrasound (HIFU) produces immediate focal lesions. Previously we have reported on the feasibility of creating thermal lesions by HIFU in in-vitro cardiac tissues. The purpose of this study was to evaluate the possibility of creating targeted and focused myocardial lesions in beating dog hearts.
Methods: The operating frequency of the transducer was 4.67 MHz, and the focal zone was 10mm depth × 1.1 mm wide at a distance of 25 mm from the transducer tip. Two dogs were anesthetized and underwent a left sided thoracotomy. The left ventricular surface was coupled with the transducer surface using echotransmission gel and water bath. The timing of the HIFU discharge was set during diastole (0.2 sec before the R wave) using an ECG triggering system newly created for this purpose. The focal point was set at the middle of the left ventricular (LV) anterior wall using conventional 2D echocardiography. Ultrasound energy was delivered at an acoustic intensity of 26.9kW/cm^2 for 0.2 seconds. For each dog and in-vitro cardiac tissue, we created 5 lesions twice (ablations were performed 10, 15, 20, 25, and 30 times for each lesion, respectively). Lesion size was assessed by measuring it's length and width.

Results: All lesions were clearly visible in each canine heart. The mean lesion size of in-vitro cardiac tissue was 13.0±2.3, 22.0±4.2, 30.2±4.8, 33.0±5.3, and 34.3±3.2 mm^2 respectively. The mean lesion size of in-vivo dog hearts was 8.5±4.2, 16.2±5.3, 23.0±9.4, 30±3.2, and 33±5.3 mm^2, respectively. There was no statistical difference in lesion size between each study, however, the in-vivo lesions tended to be smaller.
Conclusion: HIFU can be used to create targeted, well-demarcated thermal lesions in the ventricular myocardium during cardiac contraction. HIFU may allow for a noninvasive approach to ablation of cardiac tissues in many disease processes.

1168-163 High Frequency Ultrasound Thrombolysis: In Vitro Effects of Ultrasound Mode, Duration, Temperature, and Frequency

Simon T. Schaefer, Stefan Kliner, Uwe Nixdorff, Ivan Lucic, Hans Kaarmann, Werner G. Daniel, Frank A. Flachskampf, Med.Klinik II, Universitaetsklinikum Erlangen, Erlangen, Germany, Siemens AG Med.Solutions, Erlangen, Germany

Background: physical factors influencing ultrasound thrombolysis efficacy are incompletely understood.
Methods: a diagnostic echo transducer was operated by a pulse generator and an amplifier to insonate freshly obtained human blood clots after storage for 4 h at 8° C (mean mass 495± 235 mg). Clots were positioned in a water bath in the focal zone at 7.5 cm from the transducer distance and precision-weighed before and after insonation. Thrombolytic efficacy was expressed as percent baseline thrombus mass ablation. Control clots were positioned in the same experimental setup, but not insonated. Insonation time was 10-60 min. Ultrasound frequency varied 2-4.5 MHz. Ultrasound intensity in the focal zone measured by a hydrophone varied 6.5-90 W/cm2 (spatial peak temporal average). Continuous wave mode was compared to pulsed wave mode with duty cycles of 1:100, 1:50, and 1:10. 20° C versus 37° C temperature and tap water bath versus saline bath were also compared. For each combination of factors, at least five clots exposed to insonation were compared to five control (not insonated) clots.
Results: in a total of 147 experiments, ultrasound ablated thrombi with an average efficacy of 46% versus 27% in 147 controls (p<0.0001). Efficacy varied directly with output power (p<0.01) and insonation time (r=0.81, p<0.01), increased with increasing duty cycle and was highest with continuous wave ultrasound (p<0.01). A temperature of 37° C and saline were more effective than 20° C and tap water, respectively (each p<0.05). Corrected for focal zone intensity, thrombolytic efficacy was inversely dependent on ultrasound frequency (r=-0.72, p<0.001).
Conclusions: ultrasound in the 2.0-4.5 MHz frequency range ablates fresh thrombus at a distance without the use of adjuvant thrombolytic or contrast agents. The thrombolytic efficacy depends directly on mode of operation, duration and inversely on the frequency of insonation.

1168-164 Relation of Diastolic Strain Measurements by Doppler Echocardiography to Myocardial Structure and Function in Healing Canine Infarcts: Implications for the Assessment of Myocardial Viability

Tae-Ho Park, Sherif F. Nagueh, Dirar S. Khoury, Helen A. Kopelen, Spyridon Akrivakis, Kamal Nasser, Guofeng Ren, Nikolaos G. Frangogiannis, Baylor College of Medicine, Houston, TX

Background Assessment of regional diastolic function by strain Doppler imaging is a new promising technique. However, the hemodynamic and structural determinants of these measurements have not been adequately examined.
Methods Sixteen dogs underwent LAD (n=8) or circumflex (n=8) occlusion. All animals were imaged at baseline, acutely and 1-8 weeks post infarction (MI). In 10 dogs, invasive hemodynamic monitoring with a conductance catheter placed in the left ventricle (LV) was performed at the above time points. Dobutamine was infused post MI to examine LV contractile reserve. Histopathological analysis was performed on all animals (n=16) to determine the extent of interstitial fibrosis as well as the cellular and fibrillar interstitial changes post MI. ResultsAcutely and at 1-8 weeks post MI, diastolic strain rate measurements (in radial and longitudinal planes) decreased significantly (44% and 65%, respectively, p<0.01) in the distribution of the diseased artery and were significantly (correlation shown for radial and longitudinal strain rate) related to: tau (r=-0.74 ; -0.9, p<0.01), end systolic wall stress (r=-0.72 ; -0.9, p<0.01), stroke volume (r=0.78 ; 0.9, p<0.01), filling pressures (r=0.59 ; 0.62, p<0.01) and the ratio of cellular infiltration to collagen accumulation (r=0.81 ; 0.88, p<0.01). Among several indices of systolic and diastolic function, diastolic strain rate during dobutamine infusion readily identified segments with >20% transmural infarction and related best to the extent of interstitial fibrosis (r=-0.86, p<0.01).
Conclusions
Diastolic strain rate measurements are dependent on LV preload, afterload, tau, stroke volume and myocardial structure. In an animal model of healing canine infarcts, diastolic strain rate by Doppler appears to be a promising novel index of myocardial viability.

POSTER SESSION

1169 The Detection of Myocardial Fibrosis, Necrosis, and Inflammation by Magnetic Resonance Imaging

Tuesday, March 09, 2004, 3:00 p.m.-5:00 p.m.
Morial Convention Center, Hall G
Presentation Hour: 4:00 p.m.-5:00 p.m.

1169-151 Prediction of Reversible Left Ventricular Dysfunction: Comparison of Contrast-Enhanced Magnetic Resonance Imaging and Thallium-201 SPECT

Matthias Regenfus, Robert Krähner, Christian Schlundt, Johannes von Erffa, Michaela Schmidt, Niels Oesingmann, Günther Platsch, Torsten Kuwert, Werner G. Daniel, Friedrich-Alexander-Universität Erlangen-Nürnberg, Erlangen, Germany

Background: Contrast-enhanced (ce) magnetic resonance imaging (MRI) has been shown to assess myocardial viability. We compared ce MRI and Thallium-201(Tl-201) single photon emission computed tomography (SPECT) to predict reversibility of left ventricular (LV) dysfunction.
Methods: 57 patients (pts) with LV dysfunction (EF 39±13%) were examined. Functional cine studies and ce images were acquired. Rest-redistribution SPECT was performed. 32 pts had suffered acute myocardial infarction (MI) and were examined with follow-up cine MRI studies 9 months after MI. The other 25 pts showed chronic LV dysfunction and were repeatedly examined 9 months after revascularization. A 17-segment model was analysed for MRI and SPECT. Segmental hyperenhancement (HE) for MRI and tracer uptake for SPECT were quantified. For MRI, segments were considered to be viable if showing less than 25% segmental HE, for SPECT, if more than 60% Tl-201 uptake. Functional recovery in the follow-up MRI was correlated with prediction of viability by both imaging modalities. LV ejection fraction (EF) for both MRI scans was determined.
Results: In pts with acute MI, 151 of 255 (59%) dysfunctional segments showed improved wall motion with follow-up MRI. In these pts, ce MRI showed a sensitivity (sens) of 93%, a specificity (spec) of 91%, and an accuracy (acc) of 92% to detect viable myocardium, whereas SPECT a sens of 87% (p=0.3), a spec of 58% (p=0.0008), and an acc of 66% (p=0.003). In pts with chronic LV dysfunction, 79 of 161 (49%) revascularized dysfunctional segments improved. In these pts, ce MRI exhibited 94% sens, 95% spec, and 94% acc for detection of viable myocardium as compared to 86% sens (p=0.7), 56% spec (p=0.002), and 68% acc (p=0.006) for SPECT. Increase of LVEF >5% was shown in 13 (41%) pts with acute MI, and in 10 (40%) pts with chronic LV dysfunction. Multivariate regression analysis identified the dysfunctional-but-viable ratio by ceMRI as the only predictor of increase in LVEF >5%(p<0.05), whereas the equivalent by SPECT was not predictive.
Conclusion: Ce MRI, compares favorably to Tl-201 SPECT for prediction of regional and global improvement of dysfunctional myocardium in the setting of acute and chronic myocardial ischemia.

1169-152 Clinical Evaluation of Patients With Suspected Coronary Artery Disease Using a Multimodality Stress Magnetic Resonance Imaging Protocol

Igor Klem, John F. Heitner, Dipan J. Shah, Sherrie Spear, Michael H. Sketch, Jr., Michele A. Parker, Michael Elliott, Peter Cawley, Udo Sechtem, Robert M. Judd, Raymond J. Kim, Duke University Medical Center, Durham, NC

Background Stress perfusion MRI (pMRI) requires high temporal resolution which limits image quality and potentially introduces artifacts. We hypothesized that a clinically feasible stress MRI protocol including cine and contrast enhancement MRI (ceMRI) results in improved diagnostic accuracy.
Methods We prospectively enrolled 69 consecutive pts (age 58.5±11.2 yrs, 29 F) without history of cardiac disease referred for coronary angiography (CA). Cine MRI, ceMRI, adenosine and rest pMRI was performed in 62 pts within 24 hrs prior to CA. For pMRI, a SR GRE-EPI sequence was used (109 msec / slice; 4-5 slices per heart beat; 0.0625 mmol/kg Gd). All MRI studies were randomized into a pool including 30 control pts and analyzed qualitatively, blinded to pt identitiy, as follows: pMRI alone, cine alone, ceMRI alone, and incorporating all 3 sets of MRI data. Coronary artery disease (CAD) was defined as stenosis ≤ 70% on CA.
Results The sensitivity, specificity and diagnostic accuracy of pMRI, cine, and ceMRI alone are shown in the table. The multimodality analysis had the highest accuracy which was significantly improved (P=0.02) compared to pMRI alone. Specificity was improved by the recognition that matched stress and rest pMRI defects in the absence of corresponding hyperenhancement on ceMRI were artifacts and not true perfusion defects.
Conclusion A clinically feasible, multimodality stress MRI protocol has a significantly higher diagnostic accuracy compared to stress perfusion MRI alone for the detection of CAD.

	Sensitivity	Specificity	Accuracy
pMRI alone	80 %	68 %	73 %
Cine alone	52 %	62 %	58 %
ceMRI alone	40 %	97 %	74 %
Multimodality	84 %	89 %	87 %